Diatomic molecule under pulsed field: One-dimensional versus full-dimensional studies

J. T. Lin and D. S. Chuu
Department of Electrophysics, National Chiao Tung University, Hsinchu, Taiwan 30050

T. F. Jiang*
Institute of Physics, National Chiao Tung University, Hsinchu, Taiwan 30050

(Received 16 March 1998)

This work investigates the dissociation dynamics of a diatomic molecule under the chirped pulse with the vibrational and rotational degrees of freedom. Results obtained herein are also compared with those of the conventionally used one-dimensional (1D) model. According to the comparison, the 1D model still provides valuable information such as dissociation dynamics. Meanwhile, predictions such as harmonic generation spectrum from the 1D model are impractical. [S1050-2947(98)07009-7]

PACS number(s): 42.50.Hz, 31.15.Qg, 31.70.Hq

I. INTRODUCTION

The one-dimensional (1D) model for a diatomic molecule is frequently employed to examine molecular behavior under the interaction of a light field. However, a majority of these studies have neglected the rotational effect and the coupling between rotational and vibrational states. The 1D model also assumes that the molecular axis is perfectly aligned with the external field throughout the interaction time and is much easier to calculate than the full-dimensional study. Therefore the 1D model is occasionally viewed as made for computational convenience only [1]. In addition, relatively few full-dimensional calculations [1–3] are available in previous literature. Therefore closely examining the 1D model and the full-dimensional studies involving the interaction of a diatomic molecule with light pulse is a worthwhile task. In this study we demonstrate that although rather simplified, the 1D model occasionally provides valuable information regarding the dissociation behavior.

The coherent control of the molecular photoexcitation has received increasing interest recently [1,4–10]. The extent to which chirped pulses excite the 1D model of a diatomic molecule has also attracted much attention. A recent study has indicated that the threshold laser intensity for significant dissociation with chirped pulse has been reduced to around 10^{12} W/cm^2. Under such a circumstance, the ionization process can thus be neglected [4,5,9,10]. Investigations also used femtosecond chirped pulses to excite the inert gas atoms and produce higher harmonics than expected [11–15]. We have elucidated the detailed dissociation dynamics of a 1D diatomic molecule recently [16]. We explore herein the prominent rotational effects.

The rest of this article is organized as follows. Section II describes the formulation and numerical method proposed herein. Results and discussions are presented in Sec. III. Conclusions are finally made in Sec. IV.

*Author to whom correspondence should be addressed: URL: http://www.phys.nctu.edu.tw/~jiang/

II. FORMULATION AND CALCULATION

Initially studied herein are the quantum dynamics of diatomic molecule HF under the interaction of a chirped pulse. Under the Born-Oppenheimer approximation, the vibrational and rotational states in the ground electronic state can be described by the Hamiltonian

$$\hat{H}_0 = \frac{-\partial^2}{2\mu\partial R^2} + \frac{\hat{L}^2}{2\mu R^2} + D_e[1-e^{-\alpha(R-R_0)}]^2. \qquad (1)$$

To model the HF molecule, the potential parameters $D_e = 0.225$, $\alpha = 1.1741$, $\mu = 1744.8423$ and $R_0 = 1.7329$ are used, where R denotes the relative coordinate of the atomic nuclei and μ represents the reduced mass of atoms H and F. The atomic units are used hereafter unless otherwise stated. Omitting the rotational term $\hat{L}^2/2\mu R^2$ reduces the system into the 1D model. In addition, the unperturbed Hamiltonian supports 24 vibrational states; rotational levels are associated with each vibrational state as well.

The electric field of the chirped pulse can be expressed as

$$\mathbf{E}(t) = \mathbf{E}_m U(t) \sin[\Omega_c(t) t], \qquad (2)$$

where

$$\Omega_c(t) = \Omega_0 \left[1 - \alpha_n \left(\frac{t}{T_0} \right)^n \right]. \qquad (3)$$

We select the initial frequency $\Omega_0 = 1.1\omega_{12}$, where ω_{12} is the resonant frequency of the ground and the first excited vibrational levels. Also for convenience, $2\pi/\Omega_0$ is defined as the optical cycle. In addition, the fact that the vibrational energy level spacing gradually decreases from lower to higher levels accounts for why the blue to red chirping in Eq. (3) provides a climbing ladder for the pumping process. Our previous study of chirped excitation in the 1D model [16] demonstrated that the quadratic chirping [$n=2$ in Eq. (3)] is more efficient in dissociation than linear chirping [$n=1$ in Eq. (3)]. However, using linear chirping to ensure the experi-

mental feasibility [17] is a more practical measure. The envelope function $U(t)$ used to model the pulse shape is expressed as

$$U(t)=\begin{cases} t/t_0 & \text{for } t\leqslant t_0 \\ 1.0 & \text{for } t_0<t\leqslant T_0-t_0 \\ (T_0-t)/t_0 & \text{for } T_0-t_0<t\leqslant T_0, \end{cases} \tag{4}$$

where T_0 denotes the total pulse duration, and the rising time and switching-off time t_0 are set to ten optical cycles. For the field linearly polarized along the z direction, the time-dependent Schrödinger equation is

$$i\hbar\frac{\partial}{\partial t}|\Psi\rangle=\left(\frac{\hat{\mathbf{P}}^2}{2\mu}+\hat{V}_l(R)-q_e\mathbf{E}(t)\cdot\mathbf{R}\right)|\Psi\rangle, \tag{5}$$

where the effective potential is $\hat{V}_l(R)=D_e[1-e^{-\alpha(R-R_0)}]^2+l(l+1)/(2\mu R^2)$. The effective charge q_e is taken to be 0.31. For the 1D calculation, we set the rotational angular momentum l to zero and take $\theta=0$ in the above equation. While comparing our results with those in previous literature, we merely use the linear form of the dipole function as a model study despite the fact that a more practical form can be found [1,18]. In a related study, Yuan and Liu compared the dissociation behavior of a 1D model NO molecule with linear and realistic dipole functions [10].

The above time-dependent system is propagated by the split-operator algorithm [19]:

$$\begin{aligned}\psi(t+\Delta)=&\exp[-i(\hat{P}^2/4\mu)\Delta]\exp[-i\hat{V}_l(R)(\Delta/2)]\\ &\times\exp[iq_eE(t)R\cos\theta\Delta]\exp[-i\hat{V}_l(R)(\Delta/2)]\\ &\times\exp[-i(\hat{P}^2/4\mu)\Delta]\psi(t)+O(\Delta^3),\end{aligned} \tag{6}$$

where symbolically $\hat{p}=-i\partial/\partial R$. We expand the state function in partial waves:

$$\psi(R,\Omega;t)=\sum_{l=0}^{l_{\max}}F_l(R;t)Y_{l,m}(\Omega). \tag{7}$$

The state function is transformed alternatively between coordinate and momentum space by the fast-Fourier-transform method [20]. For the linearly polarized field, the magnetic quantum number is conserved and hence the system is actually two dimensional. In addition, the propagation of the dipole coupling term can be analytically solved. Since

$$e^{\pm ikR\cos\theta}=\sum_{n=0}^{\infty}(\mp i)^n\sqrt{4\pi(2n+1)}j_n(kR)Y_{n,0}(\Omega), \tag{8}$$

the following expansion can be made:

$$e^{\pm ikR\cos\theta}\psi(R,\Omega;t)=\sum_{l=0}^{l_{\max}}G_l(R;t)Y_{l,m}(\Omega). \tag{9}$$

Then, the time-dependent radial part becomes

$$\begin{aligned}G_{l'}(R;t)=&\sum_{n=|l-l'|}^{n=l+l'}\sum_{l=0}^{l_{\max}}(-1)^m(\pm i)^n(2n+1)\\ &\sqrt{(2l+1)(2l'+1)}j_n(kR)\times F_l(R;t)\begin{pmatrix} l' & n & l\\ 0 & 0 & 0\end{pmatrix}\\ &\times\begin{pmatrix} l' & n & l\\ -m & 0 & m\end{pmatrix},\end{aligned} \tag{10}$$

where

$$\begin{pmatrix} l_1 & l_2 & l_3\\ m_1 & m_2 & m_3\end{pmatrix}$$

is the Wigner 3-j symbol [21], $\Omega=(\theta,\phi)$, $k=|E(t+\Delta/2)|\Delta$ and $j_n(kR)$ is the spherical Bessel function of order n.

During the calculation, an adaptive method is applied for the 1D calculation. A range of 15.7 a.u. and 256 mesh points are initially used. Whenever the wave function hits the outer boundary, we increase the coordinate range and grid points [16]. For the full-dimensional calculation, under the intensity of 10^{13} W/cm^2 and 300 optical cycle pulse studied herein, a range of radial coordinate 46 a.u., 1024 grid points, and 45 partial waves in angular expansion are used. A filter is placed at the outer coordinate boundary. The portion filtered out is about 4% at the end of the pulse. Also, the population of the highest angular momentum partial wave is less than 10^{-4}. In the field-free calibration, the norm of wave function is accurate to the eighth decimal place during 300 optical cycles.

The dissociation probability $P_d(t)$ is defined as

$$P_d(t)\equiv 1-\sum_{\nu=1}^{24}\sum_{l=0}^{l_{\max}}P_{\nu,l}(t), \tag{11}$$

where $P_{\nu,l}(t)=|\langle\phi_{\nu,l}(t)|\psi(t)\rangle|^2$ denotes the population of the lth-rotational level of the νth-vibrational state at time t.

The alignment of the molecule with the external field has received extensive attention. Herein, we calculate the alignment probability for a certain angle θ_a as

$$\begin{aligned}P_{\text{align}}=&2\pi\int_0^{\theta a}|\psi(R,\theta;t)|^2dR\sin\theta d\theta\\ &+2\pi\int_{\pi-\theta_a}^{\pi}|\psi(R,\theta;t)|^2dR\sin\theta d\theta.\end{aligned} \tag{12}$$

The time history of alignment probability provides further information regarding the rotational motion.

III. RESULTS AND DISCUSSION

In the following, we compare the results of a 1D and a full-dimensional HF under the dipole interaction. According to the comparison, the external chirped pulse intensity is 10^{13} W/cm^2, $\Omega_0=1.1\omega_{12}$. The pulse duration T_0 is 120 optical cycles ($\sim$917 fs) for the 1D model and is 300 optical cycles ($\sim$2.3 ps) for the full-dimensional case. The chirping is linear with $\alpha_1=0.5$ for both cases. In addition, the system is initially prepared in the ground state $\nu=1$, $l=0$.

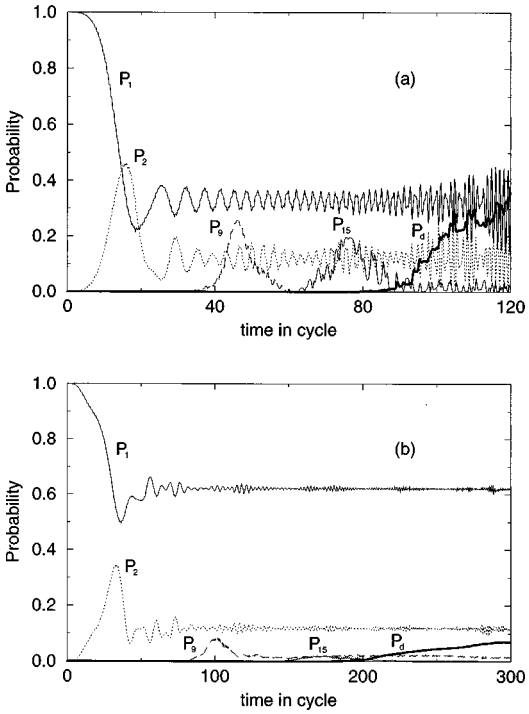

FIG. 1. Population history of some vibrational states under the linear chirping pulse of intensity 10^{13} W/cm^2, $\alpha_1=0.5$, initial frequency is $1.1\omega_{12}$. (a) One-dimensional results with pulse length 120 optical cycles. (b) Full-dimensional results with pulse length 300 optical cycles.

Whether or not the 1D calculation is valid for the important rotational degree of freedom having been totally neglected is of relevant interest. Therefore we compare the dissociation behaviors of the 1D model and full-dimensional calculation first. Figures 1(a) and 1(b) depict the population history of some vibrational states for 1D and full dimension (summed over all rotational states to each vibration level), respectively. Although the detailed dissociation dynamics differ from each other for the two cases, the corresponding excited states appear at roughly the same position if we scale the time by the total pulse duration, respectively. Consider a situation in which the motion of the 1D molecule moves in the field direction only while the real diatomic molecule has a further degree of rotation; the correspondence is not meaningless. The time lag of the arising of the 3D excited states with respect to the 1D model can be accounted for by the matrix elements described below. The 3D dipole matrix element $M^{3D}_{\nu+1,l';\nu,l}=\langle \nu+1,l'|R\cos\theta|\nu,l\rangle$ is related to the 1D matrix through

$$M^{3D}_{\nu+1,l';\nu,l}=\left(\frac{l+1}{\sqrt{(2l+3)(2l+1)}}\delta_{l',l+1}+\frac{l}{\sqrt{(2l+1)(2l-1)}}\delta_{l',l-1}\right)M^{1D}_{\nu+1,\nu}, \quad (13)$$

where $M^{1D}_{\nu+1,\nu}=\langle \phi_{\nu+1}|R|\phi_\nu\rangle$ denotes the 1D dipole matrix element between neighboring states. The magnitude of $M^{3D}_{\nu+1,l';\nu,l}$ is at most $1/\sqrt{3}$ of $M^{1D}_{\nu+1,\nu}$. Besides, rotational selection rules discourage the transitions. We can thus infer that the effect of the rotational degree of freedom in a 3D molecule reduces the alignment along the field in comparison to the 1D model. In addition, a factor of about 3 times duration is deemed necessary to arrive at the same vibrational excited state.

To further understand the dissociation dynamics, we plot the coarse-grained Wigner (CGW) density for both 1D and real HF under the chirped pulse. The CGW is defined as [22]

$$\rho_H(\langle r\rangle,\langle p\rangle;t)=(1/2\pi\hbar)|\langle \phi_{\langle r\rangle,\langle p\rangle}|\psi\rangle|^2, \quad (14)$$

where $\phi_{\langle r\rangle,\langle p\rangle}$ is the minimum uncertainty wave packet

$$\phi_{\langle r\rangle,\langle p\rangle}(R)=\frac{1}{[2\pi(\Delta r)^2]^{1/4}}\exp\left(\frac{i}{\hbar}\langle p\rangle R-\frac{(R-\langle r\rangle)^2}{4(\Delta r)^2}\right). \quad (15)$$

The real HF wave function in this study is two dimensional. Therefore we take the z-directional wave function $\psi(R,\theta=0;t)$ in the calculation of CGW to compare with the 1D case. Figure 2 displays the CGW of the 1D case at the mo-

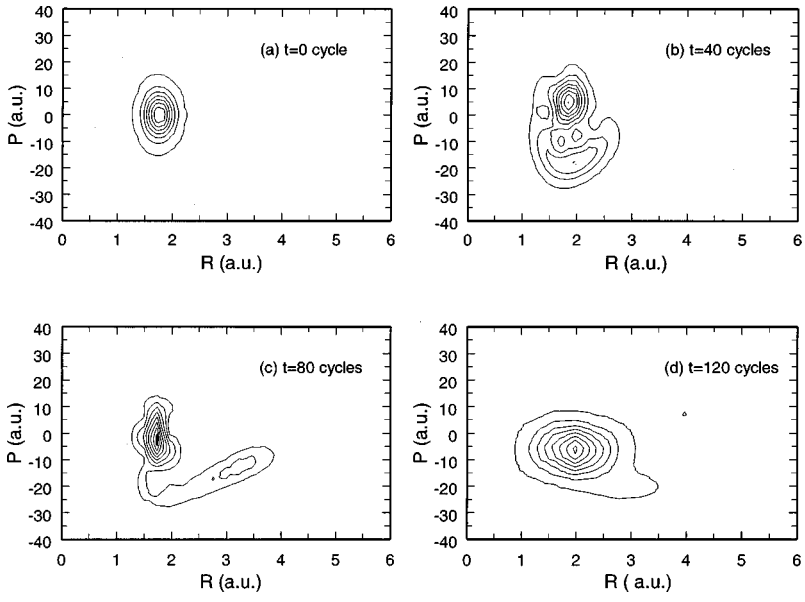

FIG. 2. Coarse-grained Wigner density plot of 1D model under the chirped pulse. The density levels linearly decrease from the inner to outer contour.

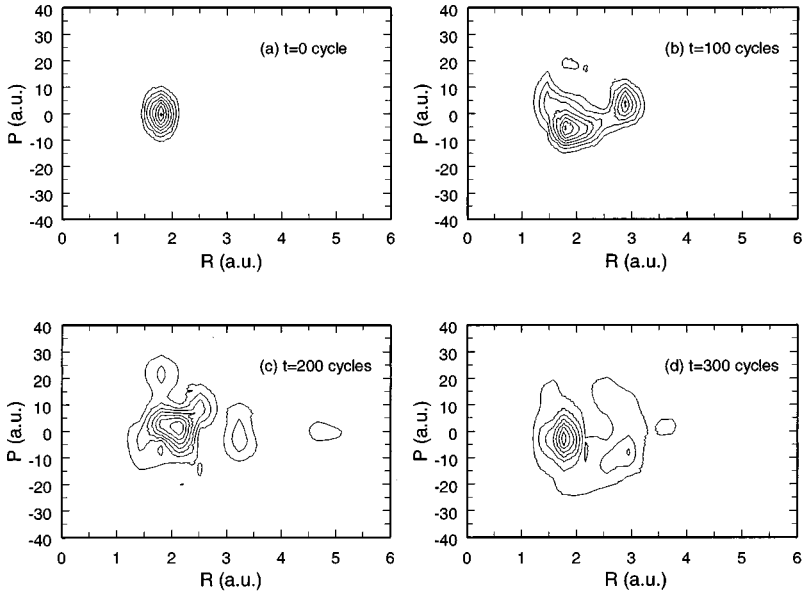

FIG. 3. Coarse-grained Wigner density plot of real HF under a chirped pulse. The density levels linearly decrease from the inner to outer contour.

ments of 0, 40, 80, and 120 optical cycles. The density levels decrease linearly from the inner to the outer contours. Figure 3 illustrates the correspondence in the real HF case, but at the moments of 0, 100, 200, and 300 optical cycles. Although they are 1D and 2D systems, respectively, their flows in phase space density closely resemble each other if the time in each case is scaled again by the total pulse duration, respectively.

Also investigated herein is the alignment of a realistic HF under linear polarized light, where P_{align} is defined in Eq. (12). For the field-free condition, the angular distribution of probability is spherically symmetric, $P_{\text{align}}=3.4\%$ for $\theta_a=\pi/12$, and $P_{\text{align}}=13.4\%$ for $\theta_a=\pi/6$. Figure 4 plots the probability P_{align} vs time for angles $\theta_a=\pi/12$ and $\pi/6$, respectively. The alignment of HF molecules under the chirped pulse of $\alpha_1=0.5$, $I=10^{13}$ W/cm^2 is unlike the dissociative ionization process in that the strong alignment arises from the fragmented ions during the interaction with a strong field ($I=10^{15}$ W/cm^2 in the experiment of Normand *et al.* on the target of CO) [23]. Nevertheless, significant alignment probability P_{align} is observed. According to Fig. 4, the alignment probability oscillates at a period of about 554 fs ($\sim$1 805 054 MHz). Comparing the period with the natural rotational frequency of HF ($\sim$1 255 400 MHz) [24] reveals that the oscillation frequency is about 1.44 times the rotational frequency. The motion is hindered rotating around the field polarization axis.

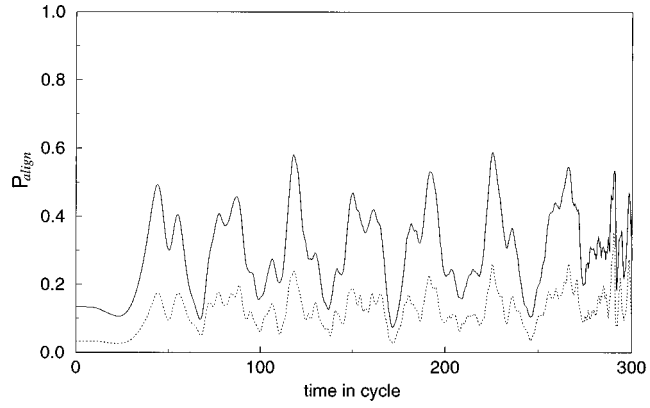

FIG. 4. Alignment probability vs time for the real HF under a chirped pulse. Dotted line is for $\theta_a=\pi/12$ and solid line is for $\theta_a=\pi/6$. For a field-free case, the probability is 3.4% and 13.4%, respectively.

Finally the harmonic generation (HG) spectra are calculated by taking the Fourier transform of the accelerated dipole moment [25] $P(\omega)=\left|1/2\pi\int_{-\infty}^{\infty}\langle\ddot{z}\rangle e^{-i\omega t}dt\right|^2$ where $\langle\ddot{z}\rangle$ denotes the quantum expectation of the accelerated dipole moment in the polarization direction and $P(\omega)$ represents the power intensity. Figure 5(a) depicts the HG spectrum of the 1D model without chirping. Figure 5(b) depicts the HG spectrum of the 1D model also but with linear chirping $\alpha_1=0.5$. Figure 5(c) depicts the HG spectrum of a real HF without chirping and Fig. 5(d) illustrates that for a real HF but with linear chirping $\alpha_1=0.5$. All the four plots are under intensity $I=10^{13}$ W/cm^2, $\Omega_0=1.1\omega_{12}$. The pulse duration is 120 optical cycles for the 1D model and is 300 optical

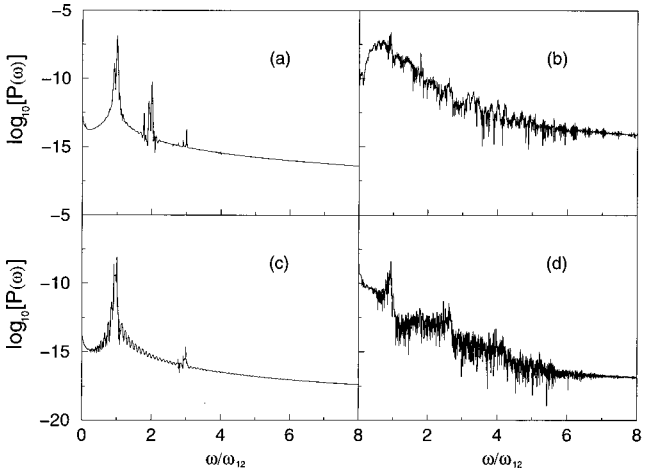

FIG. 5. Harmonic generation spectra under the field intensity 10^{13} W/cm^2, initial frequency is $1.1\omega_{12}$. The pulse length for 1D is 120 optical cycles and is 300 optical cycles for the full-dimensional case. (a) The chirping-free 1D case, (b) linear chirped 1D results, (c) chirping-free full-dimensional case, and (d) linear chirped full-dimensional spectrum.

cycles for a real HF case. Notably, in the chirping-free case, the even orders appear in 1D but disappear in 3D due to the spherical symmetry of the 3D potential [26]. There are satellite lobes located around the principal peaks coming from the rotational transition in the real HF case. Figures. 5(b) and 5(d) reveal that the spectra become broadbanded under the chirped pulse. In addition, the HG spectrum intensity of the real HF case is on the order of a magnitude smaller than the corresponding 1D spectrum. This again reveals that the rotation weakens the transition probability. Therefore simulation of the harmonic generation by the 1D model would be impractical in the molecular photoexcitation.

IV. CONCLUSIONS

This article investigates the photoexcitation of a 1D model and a real HF molecule. According to the photodissociation dynamics, although the 1D model still provides qualitative results, the time scale is about three times faster than the real case. The coarse-grained Wigner density plots display a similar tendency. Closely examining the rotational alignment with field reveals that the motion is hindered, and oscillates along the field axis slightly faster than the rotational time scale. From the time history of the alignment probability, the molecule obviously spends most of its time in the z direction on a rotational period scale. From the dipole matrix element formula, we can conclude that the rotational effect decreases the coupling strength among different states in comparing with the 1D matrix elements. Moreover, the harmonic generation spectrum from the 1D simulation is unreliable.

ACKNOWLEDGMENT

The authors thank the National Science Council of Taiwan for financial support under Contract Nos. NSC87-2112-M009-018 and NSC87-2112-M009-009.

[1] M. Kaluža, J. T. Muckerman, P. Gross, and H. Rabtiz, J. Chem. Phys. **100**, 4211 (1994).
[2] T. Seideman, J. Chem. Phys. **103**, 7887 (1995).
[3] M. V. Korolkov, G. K. Paramonov, and B. Schmidt, J. Chem. Phys. **105**, 1862 (1996).
[4] S. Chelkowski and A. D. Bandrauk, Phys. Rev. A **41**, 6480 (1990).
[5] S. Chelkowski, A. D. Bandrauk, and P. B. Corkum, Phys. Rev. Lett. **65**, 2355 (1990).
[6] B. Just, J. Manz, and I. Trisca, Chem. Phys. Lett. **193**, 423 (1992); B. Just, J. Manz, and G. K. Paramonov, *ibid.* **193**, 429 (1992).
[7] J. S. Melinger, D. McMorrow, C. Hillegas, and W. S. Warren, Phys. Rev. A **51**, 3366 (1995).
[8] S. Guérin, Phys. Rev. A **56**, 1458 (1997).
[9] W. K. Liu, B. Wu, and J. M. Yuan, Phys. Rev. Lett. **75**, 1292 (1995).
[10] J. M. Yuan and W. K. Liu, Phys. Rev. A **57**, 1992 (1998).
[11] J. Zhou *et al.*, Phys. Rev. Lett. **76**, 752 (1996).
[12] K. J. Schafer and K. C. Kulander, Phys. Rev. Lett. **78**, 638 (1997).
[13] Z. Chang *et al.*, Phys. Rev. Lett. **79**, 2967 (1997).
[14] Ch. Spielmann *et al.*, Science **278**, 661 (1997).
[15] X. M. Tong and S. I. Chu, Chem. Phys. **217**, 119 (1997).
[16] J. T. Lin, T. L. Lai, D. S. Chuu, and T. F. Jiang, J. Phys. B **31**, L117 (1998).
[17] R. B. Vrijen, D. I. Duncan, and L. D. Noordam, Phys. Rev. A **56**, 2205 (1997).
[18] R. C. Brown and R. E. Wyatt, J. Phys. Chem. **90**, 3590 (1984).
[19] M. D. Feit, J. A. Fleck, Jr., and A. Steiger, J. Comput. Phys. **47**, 412 (1982).
[20] M. D. Feit and J. A. Fleck, Jr., J. Chem. Phys. **78**, 2578 (1984).
[21] A. R. Edmonds, *Angular Momentum in Quantum Mechanics* (Princeton University Press, Princeton, NJ, 1974).
[22] S. J. Chang and K. J. Shi, Phys. Rev. Lett. **55**, 269 (1985).
[23] D. Normand, L. A. Lompré, and C. Cornaggia, J. Phys. B **25**, L496 (1992).
[24] J. D. Graybeal, *Molecular Spectroscopy* (McGraw-Hill, New York, 1988), p. 333.
[25] T. F. Jiang and S. I. Chu, Phys. Rev. A **46**, 7322 (1992).
[26] N. Ben-Tal, N. Moiseyev, and A. Beswick, J. Phys. B **26**, 3017 (1993).